Materials/Methods: 1 participant ran on a treadmill that was accelerating between speeds of 0 and 18 Km/h in 2 minutes. CODA automated motion analysis system was used to collect 3D kinematic data from 14 markers placed on the head, shoulders, elbows, wrists, hips, knees, ankles of the participant (sampling frequency 100 Hz, trial length 120 s). Marker position and acceleration data were analysed in the x, y and z directions.
Individual and combined sensor measurements were resampled at 4000Hz to generate audible waveforms. Sonograms were then computed using moving Hanning windows for all the sound signals computed for each marker and combination of markers.
Results: Sonification of individual and combined markers are shown in Figure 1. The transition between the walking and running gaits is clearly visible in all of the sonograms (Figure 1). Sonification of individual markers (Figure 1, top left) shows the frequencies underpinning the marker movement. Combining the markers, sonification shows the cancellation and enhancement of frequencies involved in the gait as a result of coupling the marker waveforms (Figure 1, top right and bottom).

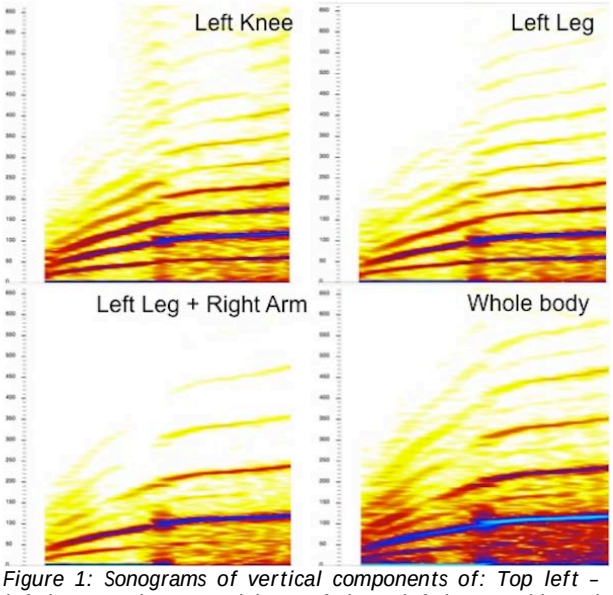

Figure 1: Sonograms of vertical components of: Top left – left knee marker; Top right – Left leg = left knee, ankle and hip markers; Bottom left – Left leg combined with Right arm = right wrist, elbow and shoulder markers; Bottom right – Whole body = combined left leg, right leg, left arm, right arm and head markers

Conclusion: Sonification provides a measure that clearly shows the phase transition between walking and running gaits. Furthermore, this measure is individual specific and situation specific. It is proposed that this method could be a used as a key tool for understanding and identifying and tracking changes in pathological or perturbed gaits; informing health practice.

Keywords: clinical gait analysis, sonification, movement analysis, coordination, biomechanical modeling

References:
[1] Exell, T.A., Irwin, G., Gittoes, M.J.R., and Kerwin, D.G. (2012). Implications of intra-limb variability on asymmetry analysis. *Journal of Sports Sciences,* 30(4), 304-309.
[2] Daffertshofer, A., Lamoth, C.J.C., Meijer, O.G., and Beek, P.J. (2004). PCA in studying coordination and variability: A tutorial. *Clinical Biomechanics,* 19(4), 415-428.
[3] Lamoth, C.J.C., Daffertshofer, A., Huys, R., and Beek, P.J. (2009). Steady and transient coordination structures of walking and running, *Human Movement Science,* 28(3), 371-386.

235
Inhibiting the actions of cathepsin L effects both tumour initiation and metastasis formation.
T.R. Wittenborn[1], P.B. Elming[1], and M.R. Horsman[1]
[1] Department of Experimental Clinical Oncology, Aarhus University Hospital, Aarhus, Denmark.

Purpose: Cathepsin L (CTSL) has been shown to play a role in tumour development and progression through its proteolytic activities. An increased expression and secretion of CTSL from cancerous cells enhances the tumour cell migration, aids in tumour invasion and promotes angiogenesis. In the present study we have investigated the role of the small molecule cathepsin L inhibitor, KGP94, on tumour initiation and metastatic spread in murine tumour models.
Methods: The C3H mammary carcinoma was implanted subcutaneously into the foot of male CDF1 mice. The SCCVII squamous cell carcinoma was either implanted into the foot or intravenously injected into the tail vein of C3H/HeNHsd mice. KGP94 was prepared by dissolving in a mixture of 10% Tween 80 and 90% HEPES-buffer. It was intraperitoneally (i.p.) injected at 0.01ml/g mouse bodyweight. Various doses (1-20mg/kg) were administered starting from the day of tumour implantation/injection. Tumour response was assessed by either determining the tumour growth time for foot tumours or the number of lung metastasis for the injections. Tumour growth time was assessed using a caliper and was the time in days to reach a volume of 500mm^3 (TGT_{500}). Lung metastasis were assessed after 2-3 weeks, where mice were euthanized, lungs were excised, weighed, and stained in Bouin's solution. Results are listed as Mean (± Standard Error). One-way ANOVA comparison of group means was performed, and a $P<0.05$ was considered significant.
Results: The TGT_{500} for control animals was 18.3 days (± 0.4) for the C3H mammary carcinoma and 13.6 days (± 0.7) for the SCCVII carcinoma. Treating the C3H mammary carcinoma with KGP94 significantly increased the TGT_{500} when doses were at 5.0 mg/kg or higher. Similar results were found with the SCCVII-carcinoma, except that a dose of 5.0 mg/kg did not have a significant effect on TGT. At lower doses of KGP94 neither of the tumour models showed significant growth delay. Studies on metastasis formation showed that 50% of animals in the control group developed metastasis within 2-3 weeks. The mean number of metastasis in these mice was 16 (±15). When mice were treated with KGP94 (10mg/kg) on a daily basis only 30% developed metastasis, and the mean number of metastasis in these mice was 5 (±4).
Conclusion: We have shown that inhibiting cathepsin L during the tumour initiation stage significantly delays tumour growth in the C3H and SCCVII murine tumour models. Furthermore, our metastasis study showed decreased metastasis formation in KGP94 treated animals. This suggests that KGP94 treatment can affect both tumour initiation and metastasis formation.

Keywords: Tumour growth inhibition; metastasis formation, cathepsin inhibitor KGP94.

236
New hypoxia probe development based on mass spectrometry
B.G. Wouters[1], L.J. Edgar[2], R.N. Vellanki[1], A.Halupa[2], D. Hedley[1], M. Nitz[2]
[1] Princess Margaret Cancer Centre, Toronto, ON, Canada
[2] University of Toronto, Toronto, ON, Canada

Many human tumors contain substantial regions of low oxygen (hypoxia), which promotes metastasis and resistance to most forms of therapy. Unfortunately, the methods available to assess cellular hypoxia are unable to detect the fluctuating oxygen concentrations that are proposed to be an important source of these cellular phenotypes, and similarly cannot detect changes in hypoxia as a consequence of treatment. We have established a novel method that enables measurement of dynamic changes in hypoxia at the cellular level. We developed a series of small molecule probes with identical chemical structures but containing different isotopes of tellurium that can be independently quantified by mass cytometry (MC) and imaging mass cytometry (IMC). This

technology allows highly multiparameter (up to 34 probes) cytometric or image based quantification of biomarkers on single cells. MC employs inductively coupled plasma mass spectrometric detection in place of the fluorescence optics used in traditional flow and imaging cytometry and circumvents the problems of spectral overlap and compensation required in fluorescence flow cytometry. The key feature of MC that we have exploited is that different mass isotopes of the same heavy metal can be independently quantified and thus used as distinct probes to allow serial measurements over time with the same chemical probe. This has allowed a series of probes that have identical pharmacokinetic profiles to be produced and used to monitor the time dependence of tumor hypoxia in both in vitro and in vivo model systems.

Keywords:
Hypoxia, imaging, mass cytometry

237

HIF-1α plays a key role in the response of HNSCC cancer stem cells to photon and carbon ion exposures

A-S. Wozny[1,2], A. Lauret[1], Y. Saintigny[3], P. Battiston-Montagne[1], M. Beuve[4], G. Alphonse[1,2] C. Rodriguez-Lafrasse[1,2]
[1] Laboratoire de Radiobiologie Cellulaire Moléculaire, EMR3738, Faculté Médecine Lyon-Sud, Université de Lyon, Université Lyon1, 69921 Oullins, France
[2] Hospices Civils de Lyon, Centre Hospitalier Lyon-Sud, 69495 Pierre-Bénite, France
[3] LARIA, CEA, DVS/IRCM au CIMAP/GANIL, 14070 Caen, France
[4] IPNL-LIRIS-CNRS-IN2P3, 69622 Villeurbanne, France

Purpose: Head and neck squamous cells carcinomas (HNSCC) have a poor prognosis due to escapement to anti-cancer therapies which leads to locoregional recurrences. The presence of cancer stem cells (CSCs), resistant to chemo- and radio-therapies, could explain these resistances and recurrences. Hadrontherapy has demonstrated favorable results for many cancers, since carbon ions induced more CSC's cell death than photons. However, for the HNSCC tumor, local control remains low. CSCs are located in a hypoxic microenvironment and hypoxia is well-known for being able to induce the epithelial mesenchymal transition (EMT). The aim of this study is to investigate the response of CSCs to radiotherapy, compared with carbon ions under hypoxic conditions. Many signaling pathways involved in the resistance of CSCs and the invasion/migration process depend on the stabilization of HIF-1α. Reactive Oxygen Species (ROS), which are produced under hypoxia and in response to irradiation, play a key role in this stabilization. However, since few data are available, the mechanisms involving ROS production, HIF-1α stabilization as well as the invasion/migration process that follows, need to be clarified in HNSCC CSCs exposed to carbon or photon radiations in a hypoxic environment.
Material and methods: Two HNSCC cells lines, SQ20B and FaDu, and their CSCs were grown in normoxic and hypoxic (1% O_2) conditions. CSCs were isolated by flow cytometry cell sorting. Cell survival curves were performed in response to photon (250kV) and carbon ion (75MeV/n, GANIL, France) irradiations in order to define the Oxygen Enhancement Ratio (OER). The expression of HIF-1α was followed by Western-Blots. ROS were quantified with a CM-H2DCFDA dye and Migration/Invasion with Boyden chambers.
Results: After photons, HNSCC cells and their CSCs appeared more resistant under hypoxia (OER>1.2) whereas the oxygen effects were cancelled after carbon ions (OER=1). Interestingly, the OER values and the expression of HIF-1α seemed to be linked. HIF-1α was weakly expressed after photon irradiation and fully inhibited after carbon ions. Additionally, under hypoxia, HIF-1α expression appeared earlier in CSCs than in the parental cell lines, confirming their adaptive properties to hypoxia. In CSCs, this expression was correlated with ROS levels. As a consequence, since HIF-1α is known to promote EMT, under normoxia as well as hypoxia, the invasion/migration abilities of CSCs were more important than in non-CSCs. Finally, after carbon ions, either in normoxic or hypoxic conditions, invasion/migration processes were decreased compared with photons.
Conclusion: HIF-1α plays a key role in the radioresistance of CSCs and in their invasiveness abilities. No expression of HIF-1α was found after carbon ion exposure suggesting that carbon ions could be a relevant therapeutic alternative to kill CSCs in their microenvironment.

Keywords: Hypoxia, Cancer stem cells, Carbon ions

238

Magnetic resonance temperature imaging in clinical hyperthermia: past experience and prospects

P. Wust[1], P. Ghadjar[1], V. Budach[1], L. Winter[2], T. Niendorf[2]
[1] Charité Universitätsmedizin Berlin, Clinic for Radiation Oncology
[2] Max-Delbrück Center for Molecular Medicine, Berlin MR Facility

Purpose: Annular phased array systems (APAS) are suitable to heat extremity, pelvic and abdominal tumors and to intensify chemo- or radiotherapy (Issels 2010). In a hybrid approach APAS and 1.5 T MR scanner were combined and clinically validated (Gellermann 2005, 2006). A review is presented regarding available technical solutions, its limitations and the potentials for further developments.
Methods: Dedicated high-frequency (filters, matching) and mechanical solutions are required for a running hybrid system shown in the upper part of the figure. This APA system has an operating frequency of 100 MHz while the MR resonance frequency is at 64 MHz (1.5 T). Gradient-echo sequences are employed to measure phase differences and extracting MR-temperatures (Gellermann 2005a). The key to obtain reliable MR-temperatures is post processing and visualization of MR datasets in a suitable software platform (here Hyperplan). Software modules has been developed for drift correction (via water bolus, calibrating probes, fat tissue), calculation and image processing of 3D MR-temperature distributions. The platform is also used for hyperthermia treatment planning (HTP) in order to compare distributions of pre-planning and online measurements. Simultaneous processing of HTP distributions and registered MR-temperature distributions has been implemented in the hybrid system in Berlin (Weihrauch 2007).
Results: The *hybrid system* was verified in a heterogeneous phantom (MR-temperature vs. direct temperature measurements, Gellermann 2005a) and clinically used for pelvic and extremity tumors under routine conditions (Gellermann 2005b, 2006). With available MR sequences (phase measurements) MR thermography is suitable for extensive fixated tumors such as sarcoma and recurrent rectal carcinoma, but not in the abdomen.
Further developments of temperature sensitive MR sequences (Winter 2016) are strongly desirable in order to correct for tissue heterogeneities (e.g. air, clips) and various forms of motion (pulsation, respiration, peristalsis, different filling in case of bladder etc.). MR thermometry of the liver is already used during thermoablation, but is a challenge for hyperthermia, where errors < 1 °C are requested.
The next technological step is an *integrated system* (lower part of the figure), where multi-antenna applicators have antennas for both heating (i.e. emitting strong phase controlled E-fields) and MR imaging (i.e. transmitting magnetic pulses and receiving the imaging signals). An experimental integrated system (7T, 298 MHz) has been implemented and tested (Winter 2013, 2015). Integrated systems are also conceivable with lower static H-fields and frequencies.
Conclusion: Current hybrid systems should be further developed to integrated multi-channel systems with increased signal-to-noise ratio and the capability of online optimization.